Density Functional Theory Calculations and Structural Studies of $(SiTe)_2(Sb_2Te_3)$ and $(CTe)_2(Sb_2Te_3)$

Justin Kang*

***Abstract*— $(SiTe)_2(Sb_2Te_3)$ and $(CTe)_2(Sb_2Te_3)$ Lattices were investigated theoretically. Structural relaxations were performed to determine optimal lattice parameters and ionic positions. Two different phases for each material were investigated and found to have stable configurations, namely the Inverted Petrov and Ferro Phases. Both structures are shown to exhibit the same phenomenon of an increase in the unit cell height in the Ferro Phase when compared to the Inverted Petrov Phase. Kohn-Sham band structures for both of these phases are calculated and qualitatively compared. $(SiTe)_2(Sb_2Te_3)$ exhibits properties that make it a potential candidate for Phase Change Memory, while $(CTe)_2(Sb_2Te_3)$ does not. The importance of spin-orbit coupling is considered for the case of the Inverted Petrov Phase $(SiTe)_2(Sb_2Te_3)$. It is shown to be responsible for the spitting of many degeneracy points, but it is also shown that the Dirac Point in the Kohn-Sham band structure can be produced without the consideration of spin-orbit coupling.**

I. Introduction

In today's "information age" the global demand for reliable and fast information storage has never been higher.[6] Currently this need is being filled by flash memory implemented with silicon-based NAND cells, which has rapidly grown into a multi-billion dollar business. This has lead to a search for smaller, cheaper, and faster alternatives. One promising alternative is Phase Change Memory (PCM). The concept of PCM takes advantage of the fact that certain materials have several metastable phases that can exist under normal operating conditions. When these phases have pronounced contrast in there electrical properties, the material phase can be used as a logic state. $(GeTe)_2(Sb_2Te_3)$ is one material being used in PCM today. It has several metastable states at room temperature with different optical and electrical properties. iPCM is a subclass of PCM where the switching process is confined to certain regions.[8] This paper includes a study of the structural stability of several materials analogous to $(GeTe)_2(Sb_2Te_3)$. $(SiTe)_2(Sb_2Te_3)$, for which cursory studied have been conducted[5] and $(CTe)_2(Sb_2Te_3)$ which has not been previously studied. Geometry relaxations for these systems are needed to determine if they can exist in analogous phases to that of $(GeTe)_2(Sb_2Te_3)$, and what the electronic properties of these systems are.

II. Simulations

In order to perform geometrical relaxations and electronic band structure calculations for the $(SiTe)_2(Sb_2Te_3)$ and $(CTe)_2(Sb_2Te_3)$ systems, Abinit[1] and ELK[7] were used, both of which are available for free under the GNU Public License.

* Engineering Physics Undergraduate Student at the University of British Columbia

A. Structural Relaxation

Structural relaxation was done entirely with Abinit, which uses a plane wave basis. The GGA exchange correlation functional as constructed by Perdew Burke and Ernzerhof (PBE) was used in the DFT self consistent field calculations. A $7 \times 7 \times 1$ k point grid was used for integration in the Brillion Zone, and a cutoff energy of 150 Ha was used. Geometry relaxations follow the structure outlined in Figure 1. Beginning with an initial set of ionic positions, the electron density is calculated using DFT, with the parameters specified above. The convergence criteria for this calculation is that the change in energy is below $\Delta E_{th} = 1 \times 10^{-5}$Ha twice in a row. Once this has been achieved, the ionic forces are calculated and the maximum force of all of the ions is determined. If this force is determined to be below the required threshold value $F = 1 \times 10^{-4}$ (atomic units), the atomic positions are considered relaxed and the process ends. If the maximum force is above the threshold a Broyden-Fletcher-Goldfarb-Shanno minimization algorithm adjusts the ionic positions and lattice parameters. These are then fed back into the DFT calculations, and the process repeats until the forces are less than the prescribed value.

B. Band Structures

Band Structures were initially calculated in Abinit, using the same pseudo-potentials described in the previous section. Abinit yielded less than desirable results and was computationally inefficient on a multi-core processor,[2] and thus the decision was made to transition to ELK, an all electron code capable of accounting for spin-orbital coupling via secondary variational techniques, and built specifically to take advantage of multi-core processors. Table 1 gives a rough breakdown of the computation time for each of the programs when running on an Intel Core i7-8550U 4 Core CPU.

TABLE I
ELK vs. Abinit time to compute 1 k-point in 1 band

Program	Time for k-point computation (s)
Abinit	3.377
ELK	1.06

The band structure and electron density calculations performed by ELK also used the GGA PBE exchange correlation functional.

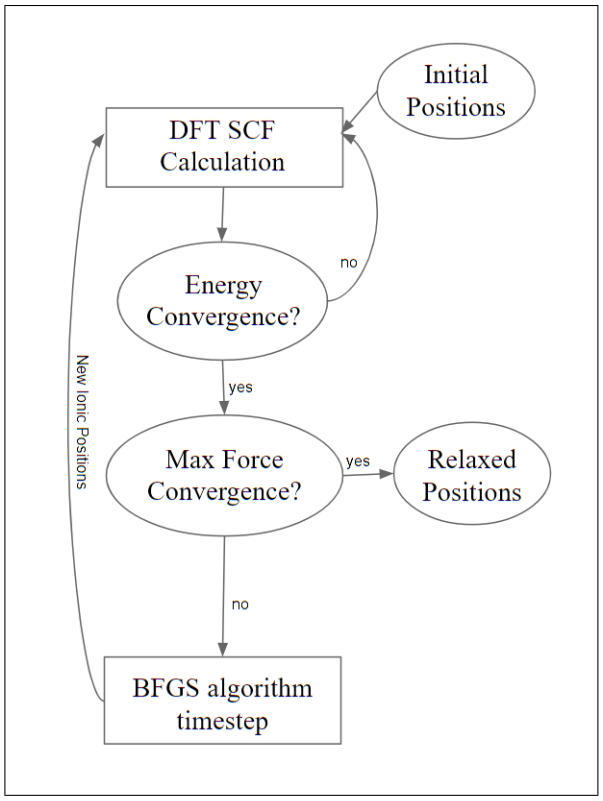

Fig. 1. Geometry optimization flow in Abinit

III. Results and Discussion

A. Results of $(SiTe)_2(Sb_2Te_3)$ Simulations

Figures 2 and 3 show two stable configurations of the $(SiTe)_2(Sb_2Te_3)$ unit cell at 0 K as determined by the geometry optimizations described earlier. Notice the lack of change in the (Sb_2Te_3) part of the unit cell in these configurations. All major differences lie in the $(SiTe)_2$ layer. This is analogous to the case of $(GeTe)_2(Sb_2Te_3)$ and means that $(SiTe)_2(Sb_2Te_3)$ has the potential to serve as a iPCM, since the difference in atomic position is associated with only a portion of the atoms in the unit cell. This has been shown to reduce entropic losses during the phase change process,[8] and results in more energy efficient switching.

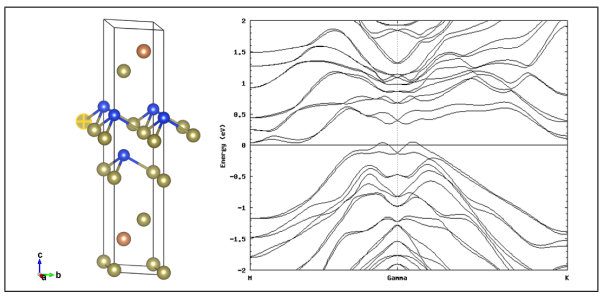

Fig. 2. Geometry optimization and Kohn-Sham band structure results for the Ferro phase of $(SiTe)_2(Sb_2Te_3)$

The band structures of the Ferro Phase and the Inverted Petrov Phase as seen in Figures 2 and 3 differ at many points on along the line from the M to Γ to K points in the first Brillioun Zone. Most notably, perhaps, at the Γ point in Figure 3, two bands meet at the Fermi Energy, and exhibit an approximately linear dispersion relation near the point of intersection. This is in stark contrast to the behavior near the gamma point at the Fermi Energy in Figure 2, where there is no intersection at the Fermi Energy. Further analysis and experimentation will have to be done to determine whether this material has sufficiently different resistivity in it's two phases.

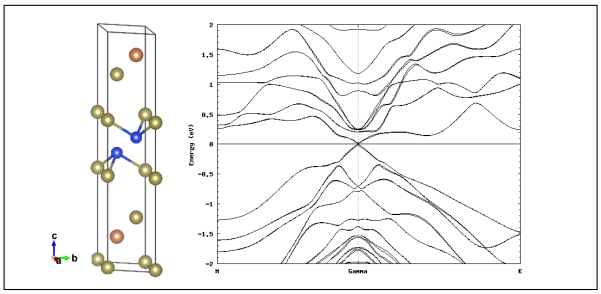

Fig. 3. Geometry optimization and Kohn-Sham band structure results for the Inverted Petrov phase of $(SiTe)_2(Sb_2Te_3)$

The Ferro Phase of $(SiTe)_2(Sb_2Te_3)$ was found to have a difference in energy of $\Delta E = +0.020$ Ha when compared to its Inverted Petrov Phase.

TABLE II
Lattice parameters of $(SiTe)_2(Sb_2Te_3)$

Parameter	Ferro	Inverted Petrov
a (Bohr)	7.888	7.773
c (Bohr)	36.331	36.098

The lattice parameters for the Inverted Petrov Phase agree with the values in literature to within 2%.[5] Lattice parameters for the Ferro Phase have not been published before. They have, however, been published for $(GeTe)_2(Sb_2Te_3)$.[6] It is observed that the Ferro phase of $(GeTe)_2(Sb_2Te_3)$ has a larger c parameter than the Inverted Petrov Phase. This phenomenon is also present in the results from the calculations from this paper for $(SiTe)_2(Sb_2Te_3)$.

B. Results of $(CTe)_2(Sb_2Te_3)$ Simulations

Figures 4 and 5 show two stable configurations of the $(CTe)_2(SbTe_3)$ unit cell at 0 K, as determined by geometry relaxations. Note that the difference between vertical distance of the $(Si-Te)$ bond is 2.62 Bohr whereas the vertical distance of the $(C-Te)$ bond is 1.94 Bohr. In contrast to the band structures of Figure 2 and 3, the band structures of Figure 4 and 5 exhibit quite similar characteristics. Both phases exhibit bands which cross the Fermi energy and are thus classified as metals.

This means that $(CTe)_2(Sb_2Te_3)$ is likely unsuitable for use in the application of Phase Change Memory. It's band structure shows that both phases considered should have similar electrical properties. This implies that determination of phase would be more difficult for $(CTe)_2(Sb_2Te_3)$ than for

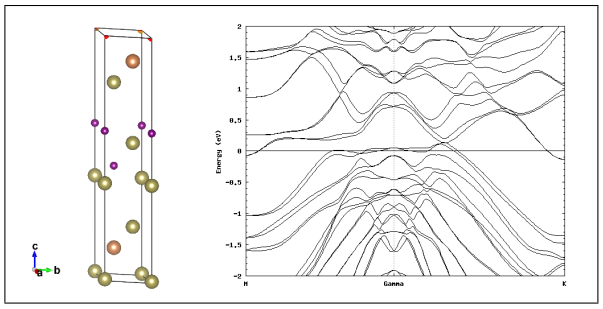

Fig. 4. Geometry optimization and Kohn-Sham band structure results for the Ferro phase of $(CTe)_2(Sb_2Te_3)$

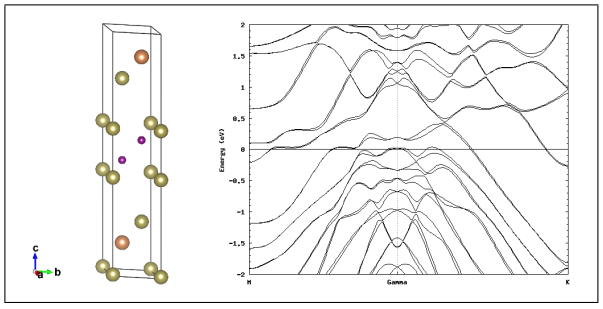

Fig. 5. Geometry optimization and Kohn-Sham band structure results for the Inverted Petrov Phase of $(CTe)_2(Sb_2Te_3)$

materials like $(GeTe)_2(Sb_2Te_3)$, a material known to have a different resistivities in the Inverted Petrov and Ferro Phases.

The Ferro Phase of $(CTe)_2(Sb_2Te_3)$ was found to have a difference in energy of $\Delta E = +0.01$Ha, when compared to the Inverted Petrov Phase.

TABLE III
LATTICE PARAMETERS OF $(CTe)_2(Sb_2Te_3)$

Parameter	Ferro	Inverted Petrov
a (Bohr)	7.215	7.268
c (Bohr)	36.271	35.586

Just as in the case of $(SiTe)_2(Sb_2Te_3)$ and $(GeTe)_2(Sb_2Te_3)$, $(CTe)_2(Sb_2Te_3)$ also exhibits an increase in lattice parameter c from the Inverted Petrov Phase to the Ferro Phase.

C. Impact of Spin-Orbit Coupling

In this section the importance of accounting for spin-orbit coupling in the systems studied is analyzed by considering one of the four systems in detail: $(SiTe)_2(Sb_2Te_3)$ in its Inverted Petrov phase. This system was analyzed by Saito et al, and spin-orbit coupling is accounted for in that work. They neglect to justify the importance of accounting for it, so this section serves as a study of that.

Figure 6 shows that SOC results in the splitting of many of the degeneracies visible in the original plot. Near the Γ point both above and below the Fermi Energy, the band structure is also visibly different.

The total energy was calculated with and without spin-orbit coupling, and the difference between the two was found to be: $\Delta E^{\text{SOC}}_{\text{total}} = 0.014$ Ha, with the spin-orbit coupled system being at the lower energy.

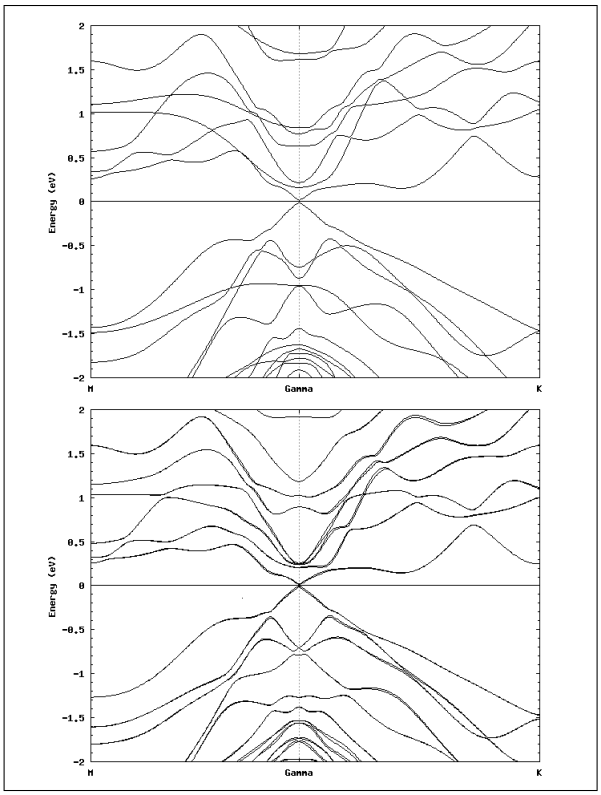

Fig. 6. Band Structure of Inverted Petrov phase of $(SiTe)_2(Sb_2Te_3)$ without Spin-Orbit Coupling (Top) and with Spin-Orbit Coupling (Bottom)

Thus it can be concluded that spin-orbit coupling is not the reason for the formation of the Dirac Point in this system, and furthermore, for a qualitative analysis of the behavior of the system at the Fermi-energy, it is not necessary to account for spin-orbit coupling in this system. If, however, the behavior of the bands above the Fermi Energy is of importance, spin orbital coupling must be accounted for, as the splitting caused by the spin-orbit coupling has a large effect.

We should be careful not to generalize this, however, as it is possible for the splitting of degeneracies to impact the behavior at the Fermi Energy in other systems.

IV. CONCLUSIONS

Density Functional Theory calculations reveal that $(SiTe)_2(Sb_2Te_3)$ and $(CTe)_2(Sb_2Te_3)$ form at least two phases. For the case of $(SiTe)_2(Sb_2Te_3)$ the Kohn-Sham band structure shows that the electronic properties of these two phases are distinct. This makes it a promising candidate for application in phase change memories. Further experimentation and synthesis of the material is necessary to make any conclusive statements. For the case of $(CTe)_2(Sb_2Te_3)$ the Kohn-Sham band structure indicates that the two phases are likely to have similar electronic properties. Further calculations, with more powerful computers, should be conducted to verify these results further, as well as synthesis and

experimentation if possible. Finally, the impact of spin-orbit coupling is analyzed in the case of Inverted Petrov $(SiTe)_2(Sb_2Te_3)$. It is shown that the linear dispersion relation near the Γ point can be retrieved even without the consideration of spin-orbit coupling. Furthermore, it is shown that the spin-orbit coupling breaks the degeneracy of many points in the Kohn-Sham band structure along the $M - \Gamma - K$ path. It is also shown to significantly modify the band structure in the region away from the Fermi Energy.

ACKNOWLEDGEMENT

I would like to thank Dr. Alireza Nojeh for allowing me to join his graduate course as an undergraduate, and for helping me develop my understanding of ab-inito and semi-empirical methods for nano-scale simulations throughout the term.

REFERENCES

[1] X.Gonze, F.Jollet, F.Abreu Araujo, D.Adams, B.Amadon, T.Applencourt, C.Audouze, J.-M.Beuken, J.Bieder, A.Bokhanchuk, E.Bousquet, F.Bruneval, D.Caliste, M.Cote, F.Dahm, F.Da Pieve, M.Delaveau, M.Di Gennaro, B.Dorado, C.Espejo, G.Geneste, L.Genovese, A.Gerossier, M.Giantomassi, Y.Gillet, D.R.Hamann, L.He, G.Jomard, J.Laflamme Janssen, S.Le Roux, A.Levitt, A.Lherbier, F.Liu, I.Lukacevic, A.Martin, C.Martins, M.J.T.Oliveira, S.Ponce, Y.Pouillon, T.Rangel, G.-M.Rignanese, A.H.Romero, B.Rousseau, O.Rubel, A.A.Shukri, M.Stankovski, M.Torrent, M.J.Van Setten, B.Van Troeye, M.J.Verstraete, D.Waroquier, J.Wiktor, B.Xue, A.Zhou, J.W.Zwanziger. Computer Physics Communications 205, 106 (2016). "Recent developments in the ABINIT software package

[2] X. Gonze, B. Amadon, P.M. Anglade, J.-M. Beuken, F. Bottin, P. Boulanger, F. Bruneval, D. Caliste, R. Caracas, M. Cote, T. Deutsch, L. Genovese, Ph. Ghosez, M. Giantomassi, S. Goedecker, D. Hamann, P. Hermet, F. Jollet, G. Jomard, S. Leroux, M. Mancini, S. Mazevet, M.J.T. Oliveira, G. Onida, Y. Pouillon, T. Rangel, G.-M. Rignanese, D. Sangalli, R. Shaltaf, M. Torrent, M.J. Verstraete, G. Zrah, J.W. Zwanziger. Computer Physics Communications 180, 2582-2615 (2009).

[3] X. Gonze, G.-M. Rignanese, M. Verstraete, J.-M. Beuken, Y. Pouillon, R. Caracas, F. Jollet, M. Torrent, G. Zerah, M. Mikami, Ph. Ghosez, M. Veithen, J.-Y. Raty, V. Olevano, F. Bruneval, L. Reining, R. Godby, G. Onida, D.R. Hamann, and D.C. Allan. Zeit. Kristallogr. 220, 558-562 (2005). "A brief introduction to the ABINIT software package."

[4] J. Tominaga ,* A. V. Kolobov ,* P. Fons , T. Nakano , and S. Murakami Adv. Mater. Interfaces 2014, 1, 1300027 "Ferroelectric Order Control of the Dirac-Semimetal Phase in GeTe-Sb 2 Te 3 Superlattices"

[5] Y. Saito*, J. Tominaga**, P. Fons, A. V. Kolobov, and T. Nakano P hys. Status Solidi RRL 8, No. 4, 302306 (2014) "Ab-initio calculations and structural studies of $(SiTe)_2(Sb_2Te_3)$n (n: 1, 2, 4 and 6) phase-change superlattice films"

[6] Zhang, W., Deringer, V., Dronskowski, R., Mazzarello, R., Ma, E., Wuttig, M. (2015). MRS Bulletin, 40(10), 856-869. "Density-functional theory guided advances in phase-change materials and memories"

[7] `http://elk.sourceforge.net/`

[8] R. E. Simpson, P. Fons, A. V. Kolobov, T. Fukaya, M. Krbal, T. Yagi & J. Tominaga Nature Nanotechnology volume 6, pages 501505 (2011)